Comparison of xenon triple point realizations

COMPARISON OF XENON TRIPLE POINT REALIZATIONS

❖ **P P M Steur[1], P M C Rourke[2], D Giraudi[1]**

[1] *Istituto Nazione di Ricerca Metrologica,*
Strada delle Cacce 91, 10135 Torino, Italy
[2] *National Research Council Canada,*
1200 Montreal Road, Ottawa, ON, K1A 0R6, Canada

E-mail (corresponding author): p.steur@inrim.it (now retired)

Abstract

It is widely recognized that the Mercury triple point being situated very close to the Water triple point constitutes a weakness in the International Temperature Scale of 1990 (ITS-90), in addition to safety concerns related to the use and transportation of Mercury. As such, a substitution for a safer, high-quality fixed point about half way between the Argon and Water triple points would be highly desirable. Now, a direct comparison is described of a Xenon cell filled in 2005 by the National Research Council Canada (NRC) and a more recently produced cell of the Istituto Nazionale di Ricerca Metrologica (INRIM). The present paper discusses the INRiM 2017 measurements on both the INRiM and NRC cells, with a follow-up measurement at NRC, and presents the difference between the two cells, (0.17 ± 0.08) mK with the uncertainties of each cell's realization of the Xenon triple point, 0.11 mK for the INRiM cell and 0.07 mK for the NRC cell (k = 1). In addition, the effect of substituting Mercury with Xenon on Type 1 non-uniqueness ("SRI," subrange inconsistency), Type 3 non-uniqueness ("NU3," cSPRT variability) and propagation of fixed point realization uncertainty is shown and discussed.

Keywords: Fixed Points; ITS-90; Triple Point; Xenon; Comparison

1 Introduction

During the development of the International Temperature Scale of 1990 (ITS-90) [1,2], it was recognized that a defining fixed point was needed between the Water triple point (WTP) at 0.01 °C and the Argon triple point (ArTP) at -189.3442 °C, and for this purpose the Mercury triple point (MTP) at -38.8344 °C was chosen [3]. Unfortunately, the temperature of the MTP is very close to that of the WTP and far from that of the ArTP, leading to an unduly high sensitivity to fixed point realization errors and scale interpolation errors [4]. These include both Type 1 non-uniqueness (also known as subrange inconsistency or "SRI," interpolation error manifesting differently in different subranges) [5, 6] and Type 3 non-uniqueness (also known as "NU3," interpolation error manifesting differently for different thermometers) [7]. Therefore, both types of non-uniqueness are expected to benefit from the use of an alternative fixed point situated about halfway between ArTP and WTP. The trend in recent years toward increasingly restrictive regulations around the transportation and use of Mercury has also spurred a search for suitable alternatives to the MTP using more benign materials [see, for example, 8-10]. Unfortunately, neither SF_6 nor CO_2 resolve the problem related to the closeness to the WTP. Instead, the Xenon triple point (XeTP) at -111.7 °C is well-positioned between ArTP and WTP and has been studied extensively since 1976 for use as a first-class fixed point for the temperature scale [11-20], but until 2005 these determinations were affected by differences of several millikelvin and melting ranges of the same size, quite unfit for a first-class fixed point.

In 2005 the National Research Council Canada (NRC) [21] showed Krypton content to be the culprit. A special batch of gas with only barely detectable Kr content resulted in very flat plateaux with a melting range within +/- 10 μK from 50% to 90% melted fraction. Isotopic effects, once a concern, were shown to be negligible. Furthermore, the XeTP was demonstrated to be highly reproducible, with a standard deviation of 48 μK over eight melts and an overall realization uncertainty of 76 μK (k = 1). Shortly thereafter INRiM also acquired a batch of gas from Spectra Gases, a commercial product produced for dark matter studies that is slightly less pure than the special batch produced for NRC. Only in 2012 a few cells of different design were sealed with this gas and using one of these, miniature cell Ec1Xe, preliminary results were published in 2014 [22]. The melt-to-melt repeatability could not yet be determined, having realized only one plateau, but the uncertainty of realization was evaluated to be 45 μK (without repeatability), quite close to the equivalent NRC value, and the

temperature difference with the published NRC value was only -0.14 mK, but the uncertainty in this INRiM temperature value is dominated by the realization uncertainties propagated from the defining ITS-90 fixed points, along with the SRI and NU3 of the scale, inflating the uncertainty up to 0.27 mK. Intrinsic uncertainty in the ITS-90 thermometer calibration due to non-uniqueness and realization uncertainties for the defining fixed points similarly inflated the uncertainty in the NRC XeTP value up to 0.32 mK. A direct comparison between cells was needed to eliminate these contributions.

Such a comparison was undertaken in 2017 at INRiM using INRiM cell Ec1Xe and NRC cell SG03, the six-thermowell Xenon cell described in section 5 of [21] (NRC cell identifier Cu-M-5). A follow-up measurement was also performed at NRC using cell SG03.

2 Experimental Apparatus and Procedures

2.1 Purity of the Xenon gas

Xenon gas in a 25 L bottle, obtained and used at INRiM to fill Ec1Xe, was sold to be of 99.9998 % purity, with a Krypton content of 0.05×10^{-6} or less. Other remaining impurities were given as 0.1×10^{-6} CO, 0.1×10^{-6} CO_2, 0.1×10^{-6} H_2O, 1×10^{-6} N_2, 0.1×10^{-6} O_2 and 0.1×10^{-6} hydrocarbons. Using the first cryoscopic constant for Xenon (A = 0.0107 K^{-1}) and the cited components, a depression of less than 0.15 mK and a maximum melting range (F = 5% to 95%) of 2.66 mK is calculated. However, estimates with the first cryoscopic constant usually result in an overestimate [23] of the plateau depression and melting range.

For cell SG03, the certificate of analysis cites the following components: 0.003×10^{-6} Kr, 0.01×10^{-6} O_2, 0.012×10^{-6} H_2O [21].

2.2 Measurements at INRiM

In 2015 INRiM took up measurements on the XeTP once again in order to corroborate the preliminary 2013 value with another set of melts with the same cell, Ec1Xe. Unfortunately, the cryocooler being in use for other projects precluded further study of the XeTP with the other two INRiM sealed cells of different design[1].

[1] Since August 2018 the leading author has retired, reducing the chances of extending the study to the other cell models even more.

Measurements were performed with the same apparatus, the same procedures and the same acquisition software as during the Neon Project [24, 25 and references therein] and during the 2012 preliminary work [22]. Helium exchange gas is used only for the initial cooldown and pumped away as soon as the triple point is reached.

For all subsequent cooling phases (re-freezing the sample between plateau realizations), cooling occurred only due to radiation and (relatively small) conduction, taking full advantage of the closed-cycle refrigerator continuously furnishing the desired thermal conditions, even when it means waiting a few days. The contribution due to the residual heat exchange while in thermal equilibrium is estimated to be 15 μK.

At temperatures of the order of 160 K, temperature control stability of the adiabatic shield was within 0.5 mK peak-to-peak. The measuring current was 0.5 mA for the (control) rhodium-iron thermometer and 1 mA for the two cSPRTs present (LN1860951 and LN1857277). These currents generate nearly the same heating power at the temperature of the XeTP, thus with little disturbance to thermal conditions on switching thermometers. All resistance values are corrected to zero measuring current. With the given measuring currents, self-heating values are less than 0.44 mK for all three thermometers. Self-heating was measured more than once on each plateau, with an average standard deviation of 4.8 μK. Applying the isotopic corrections at the *e*-H_2 and Ne fixed points in a more recent re-calibration of the cSPRTs showed the influence of these corrections not to exceed 0.05 mK at the XeTP for both cSPRTs. Noise levels on the cSPRTs were on average 10 μK ($k = 1$). Repeated measurements with the control thermometer showed the average drift during the measurement of the two cSPRTs to be on average 30 (20)[2] μK, for both cells. Only on one occasion, the worst case, these values were double.

During 2015, five valid melts were realized, while in 2017, in preparation for the comparison with cell SG03, another three melts were performed, for checking purposes. These were followed by seven melts with cell SG03. The duration of all plateaux varied between 20 and 30 hours, depending on the number of heat pulses performed. In one extreme case the plateau lasted up to 70 hours, with 16 heat pulses. Throughout the paper, F denotes the melted fraction.

2.3 Measurement at NRC

[2] Numbers in parentheses indicate one standard deviation ($k = 1$).

After the cell comparison measurements at INRiM were finished, SG03 returned to NRC where a follow-up measurement was performed using the same apparatus and procedures as the original NRC work reported in [21]. Four of the seven cSPRTs used in Section 5 of [21] remained available at the time of the present measurements: 213865, B386, 1158066 and 1820625. These thermometers were installed in the thermowells of SG03 and the ITS-90 subrange 1 fixed point calibration data from Table 6 of [21] used to calculate the temperatures of each. cSPRT 213865 was employed as the reference thermometer during the round-robin measurement ("CSPRT1" in the round-robin protocol description of [21]), and it was also continuously measured throughout the rest of the melt. 1 mA currents were continuously applied to all thermometers mounted in the cell, so that the thermal environment did not change when switching the measurement from one thermometer to the next. All cSPRT measurements have been corrected to zero measuring current.

The 2017 NRC melt plateau of cell SG03 lasted for 19 hours, with 11 heat pulses. Noise levels on the cSPRTs were on average 10 μK and the uncertainty of the cSPRT self-heating corrections determined during the round-robin measurement was on average 14 μK, both of similar magnitude to the analogous uncertainty components reported in [21]. Following the 2017 NRC melt, the Xenon sample in cell SG03 showed anomalous behaviour in subsequent melts and freezes, to be investigated in the future; however, since this event occurred after the 2017 INRiM measurements and after the 2017 NRC melt, it does not compromise the result of the cell comparison itself.

2.4 The hydrostatic effect

Whether the correction for the hydrostatic effect is to be applied or not (and to what extent), depends exclusively on the design of the cells. For this discussion it is necessary to consider the construction of both cells in detail.

Cell Ec1Xe, as all cells of type c, has a stainless-steel housing, inner diameter 10 mm, and a copper foot from which 50-70 copper wires extrude vertically into the inner parts of the cell, for a length of 35 mm. The diameter of the wires is about 0.8 mm. The gas condenses first in the space between the wires and then above them, according to the amount of gas present. See Fig. 1 (left) for a top view, showing the single wires jutting upward.

Cell SG03 is made according to NRC standard procedures, and a cut-out of a typical cell is given in Fig. 1 (right). The outer dimensions of the SG03 cell body are 76 mm length with a diameter of 32 mm. The gas condenses in the crenellated space close to the wall.

In order to calculate the effect of the weight of the liquid column (the triple point refers to melted fraction $F = 1$) one needs a) the quantity of gas sealed inside, b) the density of the liquid at the triple point [26] and c) the value of $\mathrm{d}T/\mathrm{d}p$ at the triple point [26], from which to calculate the height of the liquid column and the parameter $\mathrm{d}T/\mathrm{d}h$.

In the case of Ec1Xe the quantity of gas is known to be 5.86 g (0.04 mol); see also below. Using all the dimensional data together with items a) - c), the value for $\mathrm{d}T/\mathrm{d}h$ is calculated to be 11.78 K/m, and the height of the liquid xenon inside cell Ec1Xe is 40 mm (only 5 mm above the copper wires). However, since the high-conductivity wires in Ec1Xe dissect the liquid in many tiny slices, a temperature difference along the wires should be negligibly small so any hydrostatic head can come only from the liquid *above* the wires. The sheet of liquid above the wires is 5 mm high, equivalent to an effect of 58 μK. Possible (small) sources of uncertainty are the exact number of wires present in the cell, the fact that they are not ideally straight, and any small residual temperature difference along the wires. The residual uncertainty in the hydrostatic head correction is estimated as 5 μK.

The 2005 NRC publication [21] estimated a total hydrostatic head of 44 μK, based on a room-temperature filling pressure of approximately 2.2 MPa for cell SG03, which corresponds to 3 g of Xenon in the cell and a liquid height of 4 mm. This rough estimate of the amount of gas in SG03 is consistent with the range of experimental values of H_f found for the 2017 INRiM (49 J) and NRC (47 J) melts of this cell (see below). The 4 mm SG03 liquid height is similar to the 5 mm liquid height calculated for cell Ec1Xe above the copper wires. However, for SG03 no fine dissection of the liquid takes place, with liquid contacting only the copper wall and copper crenellations, and therefore a hydrostatic head is likely to be present. Following the 2005 paper, no correction is applied and an uncertainty contribution is taken into account equal to half the overall effect, assuming a rectangular distribution.

2.5 Estimated uncertainties

Table 1 lists the various contributions to the total uncertainty of the Xenon fixed point realization at INRiM using cell Ec1Xe (or SG03): 95 μK (or 41 μK). A contribution for the hydrostatic head of

5 μK (or 22 μK) is included according to the discussion above, as is a contribution due to chemical impurities of 84 μK (or 2 μK). When taking into account also the component due to melt-to-melt repeatability, over all melts, of 57 μK (or 58 μK), one arrives at a standard uncertainty for the triple point realization of 111 μK (or 71 μK). These values are not far from the published NRC data. Where for the INRiM cSPRTs the isotopic corrections at the *e*-H_2 and Ne triple points were explicitly taken into account, for the calibrations of the NRC cSPRTs (+80 μK and -34 μK, respectively) they were not. Considering their size with respect to the overall NRC realization uncertainty for these fixed points (200 μK each), they can be taken as uncertainties, and their propagation to the Xenon triple point temperature contributes only 3 μK. This item is therefore inserted into the uncertainty budget for SG03. The temperature values derived from the INRiM cSPRTs also carry the uncertainty related to the ITS-90 at this temperature (similarly to [5]). The uncertainty budget of the INRiM ITS-90 value near 161 K is given in Table 2, listing the contributions from fixed-point propagation, NU3 (cSPRT dependence) and SRI (subrange inconsistency) [27], leading to an uncertainty of 333 μK, obviously the dominant component. The standard uncertainty in the T_{90} values then becomes 351 μK (or 340 μK for SG03) (k = 1). This value is about three times the uncertainty associated with the realization of the fixed point, thus highlighting the improvement that can be obtained at these temperatures by substituting the XeTP in place of the MTP in the ITS-90.

For the uncertainty in the comparison of the INRiM and NRC cells, not all items contribute equally, as indicated in Table 1, leading to $u_{\text{comparison}}$ = 78 μK. An item such as "thermometer stability," *i.e.* the long-term drift over the entire campaign, does not depend on the cell used, so it is counted once. Similarly, the calorimetry is system dependent and while melt-to-melt repeatability depends critically on the calorimetry both items are to be counted once. This is corroborated by the single values for melt-to-melt repeatability being nearly equal. The term related to the thermometer calibrations (uncertainty due to isotopic composition of *e*-H_2 and Ne fixed points) cancels out in the comparison of the two cells. The terms "chemical impurities" and "isotopic composition" do not contribute in the estimate for the *measured* temperature difference, while the explicitly cell-related terms "hydrostatic correction" and "fitting[3]" have to be counted only once for each. "Electrical noise" is the thermometer noise as seen on the resistance bridge. Where in doubt whether counting twice or not, such as with electrical noise, it is decided to accept the risk of overestimating the uncertainty and count twice.

[3] The contribution due to the uncertainty of fitting $R = f(1/F)$.

The uncertainty budget of the 2017 NRC measurement is largely the same as that of the previous NRC Xenon work [21], with a few minor differences: the uncertainty of the cSPRT self-heating correction is 14 μK, rather than 7 μK; the uncertainty contribution due to the stability of the standard resistor rises from 2 μK to 16 μK when the long-term stability of the resistor since the time of the measurements of [21] is taken into account; a new propagated uncertainty of 3 μK related to *e*-H_2 and Ne triple point isotopic corrections (described above) is added; the uncertainty due to NU3 is taken as 144 μK from [27], rather than 120 μK from Fig. 6 of [21]; and a new uncertainty contribution of 74 μK due to SRI for subrange 1 [27] is added. However, these differences are small compared to the NRC realization uncertainties of the other ITS-90 fixed points propagated to the triple point of Xenon, and result in the combined standard uncertainty rising from 0.32 mK [21] to 0.34 mK.

3 Results

3.1 INRiM plateau and triple point temperature

In order to estimate influences from crystal defects at low F values and especially the possible thermal influences at high F values, the data are analyzed using a fit to 1 / F both for the central F values (30 - 75 %) only, the reduced fit, and including also the high values (30 - 95 %), the full fit. The differences between the full fit and the reduced fit (both quadratic) arrived at about 0.1 mK, while the differences of the full fit with the (linear) reduced fit were within 60 μK with an average of 20 μK, with overall smaller values for cell SG03. These numbers were then combined with the standard deviation of fit, leading to the average values given in Table 1. The differences are to be compared with the calculated effect of the residual heat flux on the $F = 1$ value of up to 15 μK. The higher differences using the quadratic reduced fit are due to the few values available to constrain the quadratic behaviour sufficiently. In all cases the full fit was used and Figures 2 and 3 show the plateaus obtained with Ec1Xe and SG03, respectively.

The W values and corresponding triple point temperatures found for the two cSPRTs and for each of the two cells are given in Table 3, along with the averages and their associated standard deviation of the mean. The difference of up to 0.23 mK between the two cSPRTs is due to ITS-90 non-uniqueness. The difference, dT_{cells}, between cells SG03 and Ec1Xe, corrected for hydrostatic head, is 0.199 mK for thermometer LN1860951 and 0.134 mK for thermometer LN1870577. The average temperature difference between the cells, considering both thermometers, is then 0.17 mK with a comparison

uncertainty ($k = 1$) of 0.08 mK. This value is to be compared with the expected temperature depression as calculated from the first cryoscopic constant of 0.15 mK (Section 2.1).

3.2 NRC plateau and triple point temperature

The shape of the SG03 melt plateau measured at NRC in 2017 using the reference cSPRT 213865 is shown as a solid line in Fig. 4, and the temperatures of all four cSPRTs from the round-robin measurement at $F = 0.65$ during the same melt, as well as that averaged over all four cSPRTs, are shown as open symbols. The temperatures of the same four cSPRTs from [21], as well as that averaged over all four of them are shown as solid symbols. For each cSPRT, the temperature is taken as the average over the round-robin measurements of that cSPRT that took place during the 8 melts described in Section 5 of [21], with the uncertainty bars representing the standard deviation of each particular cSPRT's round-robin temperatures across the 8 melts. These results are summarized in Table 4, and show that, at the time of the 2017 NRC melt measurement, both the SG03 Xenon sample and the set of cSPRTs remained consistent with the 2004 measurements reported in [21]. The SG03 curve from Fig. 2 of [21], which was measured using cSPRT 1158066, is shown as a dashed line in Fig. 4: its offset relative to the 2017 melt plateau (solid line) is consistent with the difference between cSPRT 1158066 and cSPRT 213865 (due to NU3 of the ITS-90) and melt-to-melt variability observed in [21]. The agreement of this melt with the previous work shows that the anomalous SG03 behaviour observed after this melt does not compromise the result of the comparison itself.

4 Auxiliary data

4.1 INRiM measurements

As part of the measurement procedure (see also [28] for a list of desirable experimental details), the heat capacity was measured several times in a row slightly below plateau, and the average value for Ec1Xe was 137.7 (2.3) J/K. This value is somewhat higher than the one reported in [22]. This could be due to thermal conditions being not optimal then, and heat capacity been measured only once (usually 3-4 times). For cell SG03 the value was found to be 139.1 (0.6) J/K. The coincidental agreement between the two values, within the combined uncertainties, is surprising considering the different materials and the different masses for the two cells: Ec1Xe is stainless steel with a copper insert on a copper block, while SG03 is fully made of copper with only a thin stainless steel sleeve for

mechanical support. The thermal resistance between the cell and shield, R_S, was measured by changing the shield setting (below plateau) and observing the resulting temperature drift of the cell. R_S was found to be on average 280 (12) K/W for Ec1Xe and 383.6 (6) K/W for SG03. In one case the value of R_S for cell Ec1Xe was estimated by changing the shield setting *during* the plateau and recording the temperature shift due to this change. Here a value of R_S = 251 K/W was found, not too far from the value obtained from drift change caused by shield change. The differences in R_S values reflect the variation in adiabatic conditions for the two cells. The values are relatively low with respect to the low-temperature fixed points, but it should be born in mind that vacuum is not as good at 160 K as it is at lower temperatures leading to a lower thermal resistance.

The difference in material is also reflected in the value of the thermal resistance between the cell wall and the solid, R_{CS}, as a function of melted fraction, F, see Fig. 5. R_{CS} is calculated by comparing the steady-state overheating temperature of the cell achieved while heat is being applied during a heat pulse to the relaxed cell temperature between heat pulses, taking into account the unbalanced heat load due to the applied heater power. For cell Ec1Xe, where the applied heat must pass through the s-s housing, the value of R_{CS} increases, on a logarithmic scale, monotonically from 0.1 K/W and 1 K/W, between F = 0.2 and F = 1, while for cell SG03, where the heat also must pass through the s-s sleeve but having a much higher copper content, the values are practically flat up to F = 0.8 at about 0.25 K/W, only rising up to 0.5 K/W towards F = 1. At these levels the residual heat flux of 10-15 μW raises the triple-point value by about 5 μK (SG03) and 15 μK (Ec1Xe) at F = 1. No correction was applied for this effect.

Part of the filling procedure for INRiM sealed cells is the weighing of all the cell components before and after filling. Thus the amount of gas sealed inside is known, usually about 0.04 mol. This allows the calculation beforehand of the heat of transition, H_f. Using the literature value for the molar H_f of 2315 J / mol [26], for cell Ec1Xe (with 0.0446 mol) a value of 103.3 J is obtained. From measurements an actual (average) value of 100.2 (0.9) J was found, a difference of only 3.1%, suggesting that the molar H_f value should be rather 2245 (20) J / mol. Unfortunately, no uncertainty for the literature value is given in [26]. Curiously, in [21] two different values are given, 2315 J / mol (their Section 2) [4] and 2297 J / mol (their Section 5), and it is not clear what the source of the second

[4] This value is mistakenly referred there to a paper regarding isotopic composition (reference 17 within [21]), but matches the value for Xenon listed in another reference (reference 16 within [19]; our [26]).

value is. For cell SG03 the exact value for H_f was not known beforehand, but a rough guess from the number of 2 J heat pulses applied during the prior NRC work [21] leads to a *minimum* value of about 40 J. The subsequent INRiM measurements yielded an (average) value of 49.0 (0.5) J, in agreement with the estimate. For both cells the residual heat flux (which always includes the heat from the thermometer) contributed 1-2 J, depending on the duration of the plateau.

The average melting range for the two cells, from 5 to 95%, was 2.3 (0.3) mK for Ec1Xe and 0.6 (0.4) mK for cell SG03. Here the difference is undoubtedly due to the purer gas in SG03. Curiously, while the values for Ec1Xe were rather constant from melt to melt, those for SG03 varied widely - from a minimum of 0.23 mK to a maximum of 1.25 mK - while the melting range based on the nominal purity of the gas was calculated to be 0.18 mK, close to the lowest experimental value. This could possibly reflect the influence of the inner structure of the cell (Fig. 1, right), which in principle could allow condensation at different heights, and a varying distribution from melt to melt. Heat pulses varied between shorter-stronger, longer-weaker, more-weaker and fewer-stronger pulses, not showing any real benefit from one to the other. The main drawback from either longer-weaker or more-weaker heat pulses is the increasing influence of the residual heat flux. However, weaker heat pulses have the advantage of reducing overheating thereby diminishing the risk of turning back on plateau by partially inverting the residual heat flux.

4.2 NRC measurement

As with the INRiM measurements, the heat capacity of the assembly consisting of cell SG03, its Xenon sample and the cryostat's cell holder was measured twice below the 2017 NRC melt plateau prior to initiating the melt and once above the plateau immediately after the melt was completed. The average value for the heat capacity of the assembly was 409 (2) J/K. This value is much higher than that determined at INRiM for cell SG03, and similar to the value observed for a different cell measured in the NRC cryostat [8], because the large mass of copper comprising the cell holder dominates the heat capacity of the assembly. The thermal resistance between the cell and shield, R_S, was measured in two different ways: below the melt, prior to melt initiation, the shield set point was changed and the resulting temperature drift of the cell observed; and above the melt, after melt completion, from the time constant of an exponential function fitted to the post-melt drift of the cell temperature back toward the fixed shield temperature. R_S was found to be 173 (13) K/W by the former

method, and 172 (1) K/W by the latter method. The reduced value of R_S compared to that seen in the INRiM experiments is indicative of the differing adiabaticity of the two cryostats. However, this value of R_S is approximately twice as large as that measured in the same NRC cryostat at the triple point of Sulfur Hexafluoride [8], consistent with observations at INRiM that R_S tends to increase at lower temperatures.

The experimental estimation of the thermal resistance between the metallic cell walls and the adjacent portions of the solid Xenon sample, R_{CS}, relies upon the cell temperature approaching a steady-state temperature that corresponds to the unbalanced heat load applied by the heater during each heat pulse. As in [21], the 2017 NRC melt utilized shorter-stronger heat pulses (1 minute pulse durations), such that the steady-state approximation does not hold, resulting in an underestimation of R_{CS} by an order of magnitude relative to the INRiM measurements of SG03. The thermal relaxation following each heat pulse was dominated by much slower equilibration processes between different parts of the Xenon sample, so an alternate approach in which R_{CS} is calculated from the time constant of an exponential decay function fitted to this thermal relaxation [8] yields a value that is overestimated by an order of magnitude and that is likely more representative of the thermal resistance between different parts of the solid Xenon sample.

The heat of transition H_f observed for SG03 in the 2017 NRC melt was 47 (2) J, which is similar to the values of H_f observed for SG03 in the INRiM melts and calculated from the roughly estimated 3 g of Xenon originally filled into SG03.

5 Non-uniqueness issues

As already discussed in the Introduction, a considerable improvement in both SRI and NU3 is expected from the substitution of the MTP with the XeTP. These effects have now been investigated, be it with a moderate set of seven cSPRTs using the calibration data given in [21].

5.1 Type 1 non-uniqueness (subrange inconsistency or SRI)

For SRI the same procedure was used as done for Fig. 10 in [6] (Fig. 8 in [27]). The top panel of Fig. 6 depicts the results for the ensemble of 7 cSPRTs from [21] when using the MTP, showing largely the same dependence as in [6]. In the bottom panel the XeTP was substituted in place of the MTP. It is

immediately clear that the ballooning feature between the ArTP and the MTP (< 0.45 mK) and the almost absence of SRI in the narrow interval between the MTP and the WTP (< 0.02 mK), present in the MTP case, become more evenly distributed over the whole temperature interval in the XeTP case (<0.15 mK between the ArTP and the XeTP (a reduction by 66%) ; < 0.17 mK between the XeTP and the WTP). It seems that even a minor benefit can be observed below the ArTP: a reduction by 0.02 mK at 35 K and at about 30 K.

5.2 Type 3 non-uniqueness (NU3)

For the discussion on NU3, even when only four cSPRTs could be found with the required data, *i.e.* comparison data over the full temperature range from WTP down to 24.5 K (taken from Fig. 2 of [7] and another similar unpublished measurement, as treated in the *Guide to the Realization of the ITS-90* [27]) *and* calibration data at the XeTP (from [21]), an attempt was made to calculate the effect of fixed point substitution. The NU3 data points shown in Fig. 10 of [27] were calculated using a comparison data set of 14 cSPRTs and the subrange 1 deviation function, truncated at the NeTP. These points are reproduced as open circles (labelled "ITS-90 Guide Fig. 10") in Fig. 7 of the present work.

The blue solid lines and symbols in Fig. 7 labelled "4 cSPRTs (Hg)" are calculated using the four cSPRTs that are common to both the full comparison data set [27] and [21]: 213865, B386, 1158066 and HS113. The ITS-90 fixed point calibration W and T_{90} values for these cSPRTs listed in Table 6 of [21] have been substituted into the comparison data set and deviation function, and then the same procedure used to generate Fig. 10 of [27] was applied to determine the NU3 for this small four-cSPRT ensemble. The level of agreement between the "4 cSPRTs (Hg)" curve and "ITS-90 Guide Fig. 10" curve in Fig. 7 is indicative of how representative this small subset of cSPRTs is to the larger ensemble used in [27].

The magenta dashed line and symbols in Fig. 7 labelled "4 cSPRTs (Xe)" are calculated in the same manner as the "4 cSPRTs (Hg)" curve, except that rather than substituting the MTP T_{90} and W values from the bottom line in Table 6 of [21] into the comparison data set and deviation function, T_{90} = 161.405 96 K and the measured W values at XeTP from Table 7 of [21] are substituted instead. Even with such a very modest sample size, indications can be seen of an NU3 reduction of approximately

30 % in the temperature range between ArTP and MTP, if XeTP replaces MTP. However, in order to draw any firm conclusions a larger dedicated study will be required.

5.3 Propagation of calibration errors

Using the calibration of any cSPRT calibrated over subrange 1 (NRC) or 2 (INRiM) with the XeTP instead of the MTP a change of 1 mK equivalent was applied to W(Xe) and the resulting calibration curve was compared to the original one, exactly as was done in the early 1990s for the first edition of the Supplementary Information of the International Temperature Scale of 1990 (SuppInf). The SuppInf is now updated and available as the *Guide to the realization of the ITS-90* at the website of the BIPM [27][5]. Fig. 8 shows, for the different subranges, how a 1 mK change at either MTP or XeTP propagates towards the other temperatures. Only results for one cSPRT are shown (213865), but those for all other cSPRTs are very similar. Evidently, the biggest difference occurs for subrange 4 where the reduction is slightly less than 50 %, while for subranges 3, 2 and 1 the reduction is 30 %, 20 % and 20 %, respectively. Incidentally, the maximum is reached in all cases at about the same temperature.

6 Conclusion

The XeTP is shown to be a first-class fixed point that can be used as an alternative for the MTP. It can be realized with a standard uncertainty of (0.07 – 0.11) mK. It was shown in the past that Krypton content has been a major factor in reducing its performance and this is now corroborated in the comparison between the INRiM cell and the NRC cell with extremely pure gas, see Figs. 2 and 3. However, a rather modest amount can still be afforded, as shown in this direct comparison of the two cells. Taking the (small) hydrostatic correction into account (for Ec1Xe), the difference between the two cells turns out to be (0.17 ± 0.08) mK, in agreement with the rough estimate provided by a calculation using the first cryogenic constant.

A limited study on the effect of substituting the XeTP for the MTP on SRI and NU3 shows the first to improve dramatically (by two thirds) between the ArTP and MTP, at the expense of an increase in the (very limited) temperature range between the MTP and the WTP. A test on only four cSPRTs seems to hint at an improvement also in NU3. Also regarding the propagation of calibration errors the

[5] The first edition of the SuppInf is out of print, and the new Guide does not (yet) contain such graphs.

substitution seems to offer improvements of about 20 %, 20 %, 30 % and 50 %, for subranges 1, 2, 3 and 4, respectively.

Acknowledgements

PMCR would like to acknowledge useful discussions with Ken Hill and Andrew Todd.

References

[1] Preston-Thomas H, *Metrologia* **27**, 3-10 (1990)

[2] Preston-Thomas H, *Metrologia* **27**, 107 (1990) (erratum)

[3] Crovini L, Jung H J, Kemp R C, Ling S K, Mangum B W, Sakurai H, *Metrologia* **28**, 317-325 (1991)

[4] White D R, AIP Conf. Proc. **1552**, 81-88 (2013)

[5] Steele A G, *Metrologia* **42**, 289-297 (2005)

[6] Meyer C W, Tew W L, *Metrologia* **43**, 341-352 (2006)

[7] Hill K D and Steele A G 2003 The non-uniqueness of the ITS-90: 13.8033 K to 273.16 K 8th Symp. Temperature: Its Measurement and Control in Science and Industry ed D C Ripple (New York: American Institute of Physics) pp 53–8

[8] Rourke P M C, *Metrologia* **53**, L1-L6 (2016)

[9] Tew W L, Quelhas K N, (2018) Realizations of the Triple Point of Sulfur Hexafluoride in Transportable and Refillable Cells *J Res Natl Inst Stan* 123:123013

[10] Bedford R E, Bonnier G, Maas H and Pavese F, *Metrologia* **27**, 107 (1996)

[11] Bonnier G and Malassis R, 1976 *Comité Consultatif de Thermométrie 11th Session* Document CCT/76-24

[12] Ancsin J, *Metrologia* **14**, 45-46 (1978)

[13] Inaba A and Mitsui K, 1978 *Comité Consultatif de Thermométrie 12th Session* Document CCT/78-26

[14] Kemp R C and Kemp W R G, in *Temperature: Its Measurement and Control in Science and Industr*y, Vol 5 Part 1, ed. by J F Schooley (AIP, New York), 229-230 (1982)

[15] Hermier Y and Bonnier G, in *Proceedings of Tempbeijing 1982*, 72 (1982)

[16] Zhang Guoquan and Wang Li, 1987 *Comité Consultatif de Thermométrie 16th Session* Document CCT/87-59

[17] Ancsin J, *Metrologia* **25**, 221-225 (1988)

[18] Khnykov V, Losev M I, Gerasimov G M and Astrov D N, 1989 *Comité Consultatif de Thermométrie 17th Session* Document CCT/89-8 10

[19] Head D I, Hermier Y, Rusby R L, Bonnier G and Wei Mao, in *Proceedings of Tempmeko '90*, 118-125 (1990)

[20] Pfeiffer E R and Reilly M L, in *Temperature: Its Measurement and Control in Science and Industry*, Vol 6 Part 1, ed. by Schooley J F (AIP, New York), 271-276 (1992)

[21] Hill K D and Steele A G, *Metrologia* **42**, 278-288 (2005)

[22] Steur P P M and Giraudi D, *International Journal of Thermophysics* **35**(3), 604-610 (2014)

[23] Consultative Committee for Thermometry under the auspices of the International Committee for Weights and Measures 2015 *Guide to the realization of the ITS-90: Fixed Points: Influence of Impurities* available at http://www.bipm.org/en/committees/cc/cct/guide-its90.html

[24] Pavese F, Steur P P M, Fahr M, Hermier Y, Hill K D, Kim J S, Lipinski L, Nagao K, Nakano T, Peruzzi A, Sparasci F, Szmyrka-Grzebyk A, Tamura O, Tew W L, Valkiers S and van Geel J, "Dependence of the Triple Point of Neon on Isotopic Composition and its Implications for the ITS-90," in *Temperature: Its Measurement and Control in Science and Industry*, Vol 8 Part 1, AIP Conf. Proc 1552, 192-197 (2013)

[25] Steur P P M, Pavese F, Fellmuth B, Hermier Y, Hill K D, Kim J S, Lipinski L, Nagao K, Nakano T, Peruzzi A, Sparasci F, Szmyrka-Grzebyk A, Tamura O, Tew W L, Valkiers S and van Geel J, 2012 Comité Consultatif de Thermométrie 26th Session Document CCT/12-21(rev)

[26] Pavese F and Molinar G M M, Modern Gas-Based Temperature and Pressure Measurement, 1992 (1st ed.), p. 475 and 2013 (2nd ed.), p. 535

[27] Consultative Committee for Thermometry under the auspices of the International Committee for Weights and Measures 2015 *Guide to the realization of the ITS-90: Platinum resistance thermometry* available at http://www.bipm.org/en/committees/cc/cct/guide-its90.html

[28] Fellmuth B, "New Protocol for the Realization of the Triple Points of Cryogenic Gases as Temperature Fixed Points" in: *Temperature: Its Measurement and Control in Science and Industry*, Vol 8 Part 1, AIP Conf. Proc 1552, 176-179 (2013)

Table 1 Uncertainty budget related to the Xenon triple point realization with cells Ec1Xe and SG03 at INRiM.

Item	Probability distribution	Value (Ec1Xe) / μK (k = 1)	Value (SG03) / μK (k = 1)
Resistance measurement[1)]	Normal	25	25
Calorimetry and R_{CS}[1)]	Rectangular	15	15
Thermometer stability[1)]	Normal	10	10
Electrical noise	Normal	1.5	1.5
Fitting	Normal	30	15
Thermometer self-heating	Normal	6	6
Hydrostatic head correction	Rectangular	5	22
Propagation of uncertainty due to isotopic composition at e-H_2 and Ne[2)]			3
Chemical impurities[2)]	Rectangular	84	2
Isotopic composition[2)]	Normal	2	2
u_{LP}		95	41
Melt-to-melt repeatability[1)]	Normal	57	58
u		**111**	**71**
Cell comparison (considering items [1)] only once and without items [2)])	u =	**78 μK**	

Table 2 Uncertainty budget for the realization of ITS-90 subrange 2 at 161 K, as carried on the INRiM cSPRTs.[6]

Item	Probability distribution	Value / μK ($k = 1$)
Uncertainty in the Ar TP realization	Normal	110
Uncertainty in the Hg TP realization	Normal	100
Uncertainty in the TPW TP realization	Normal	70
Propagation from the fixed points (Ar, Hg, TPW)	Normal	204
Type-3 non-uniqueness (cSPRTs)	Normal	144
Type-1 non-uniqueness (subrange)	Normal	147
u		**333**

[6] Taken from [22], with corrected values for SRI and NU3.

Table 3 Temperature values obtained for the two cSPRTs in cells Ec1Xe and SG03, respectively, from measurements at INRiM. The correction for hydrostatic effect is applied at the end (see Section 2.4). The corrected, final, temperatures are denoted by *T*(Ec1Xe) and *T*(SG03).

	Ec1Xe			**SG03**		
	Date	W	Temperature / K	Date	W	Temperature / K
LN1860951	23/10/2015	0.545 956 185	161.405 878	30/05/2017	0.545 956 498	161.405 953
	18/11/2015	0.545 955 348	161.405 690	14/06/2017	0.545 956 280	161.405 901
	28/11/2015	0.545 955 403	161.405 723	06/07/2017	0.545 956 203	161.405 882
	06/12/2015	0.545 955 541	161.405 743	15/07/2017	0.545 955 817	161.405 880
	03/04/2017	0.545 955 625	161.405 791	22/09/2017	0.545 956 136	161.405 866
	11/04/2017	0.545 955 825	161.405 766	01/10/2017	0.545 956 370	161.405 923
	18/04/2017	0.545 955 719	161.405 732			
		Mean / K	161.405 760		Mean / K	161.405 901
	hydrostatic head corrected		161.405 702	hydrostatic head corrected		161.405 901
	St.Dev.(mean) / mK		0.025	St.Dev.(mean) / mK		0.014
T(SG03) - T(Ec1Xe) = 0.199 (29[4]) mK						

	Ec1Xe			**SG03**		
	Date	W	Temperature / K	Date	W	Temperature / K
LN1857277	23/10/2015	0.545 983 011	161.406 095	30/05/2017	0.545 983 186	161.406 137
	18/11/2015	0.545 982 283	161.405 919	14/06/2017	0.545 982 982	161.406 088
	28/11/2015	0.545 982 395	161.405 946	06/07/2017	0.545 982 867	161.406 060
	06/12/2015	0.545 982 490	161.405 969	15/07/2017	0.545 982 462	161.405 962
	03/04/2017	0.545 982 698	161.406 019	22/09/2017	0.545 982 821	161.406 049
	11/04/2017	0.545 982 634	161.406 004	01/10/2017	0.545 983 029	161.406 099
	18/04/2017	0.545 982 514	161.405 975			
		Mean / K	161.405 990		Mean / K	161.406 066
	hydrostatic head corrected		161.405 932	hydrostatic head corrected		161.406 066
	St.Dev.(mean) / mK		0.023	St.Dev.(mean) / mK		0.027
T(SG03) - T(Ec1Xe) = 0.134 (35[7]) mK						

[7] From the combination of the two single standard deviations

Table 4 SG03 cSPRT round-robin measurements from 2017 NRC melt and reference [21].

cSPRT serial number	2017 NRC melt temperature / K	Reference [21] 8-melt average temperature / K	Reference [21] 8-melt temperature standard deviation / μK
213865	161.405 898	161.405 927	49
B386	161.406 042	161.406 087	50
1158066	161.406 019	161.406 059	50
1820625	161.405 821	161.405 754	61
1872182		161.405 885	46
1876687		161.406 058	49
HS113		161.405 956	42
4-cSPRT average	**161.405 945**	**161.405 957**	**52**
7-cSPRT average		**161.405 961**	**48**

Figure Captions

Fig. 1 left) A top view of the inside of a type c INRiM sealed cell, showing the presence of the copper wires.
right) NRC cell SG03 (Cu-M-5) alongside a cutout of a cell of similar design, showing the crenellated space near the wall.

Fig. 2 The shape of the plateaux obtained with cell Ec1Xe, for cSPRT s/n LN1857277, from measurements at INRiM, where R denotes cSPRT resistance and F melted fraction. $R(F = 1)$ is obtained from a fit to the experimental data, using the $1 / F$ representation (see text).

Fig. 3 The shape of the plateaux obtained with cell SG03, for cSPRT s/n LN1857277, from measurements at INRiM, where R denotes cSPRT resistance and F melted fraction. $R(F=1)$ is obtained from a fit to the experimental data (see text), using the $1 / F$ representation.

Fig. 4 Results from the melt plateau obtained with cell SG03 from the measurement at NRC in 2017. The shape of the plateau, measured using reference cSPRT s/n 213865, is shown as a solid line; round-robin measurements of four cSPRTs appear as open symbols. The SG03 curve from Fig. 2 of [21], measured using cSPRT s/n 1158066, is shown as a dashed line; round-robin measurements of four cSPRTs, averaged over the 8 melts described in Section 5 of [21], appear as closed symbols, with uncertainty bars representing standard deviations over the set of 8 melts (symbols are offset in F for clarity).

Fig. 5 Values for the thermal resistance between the cell wall and the solid sample, R_{CS}, as a function of melted fraction F - for cell Ec1Xe and cell SG03 - from measurements at INRiM.

Fig. 6 The effect on subrange inconsistency for a batch of 7 cSPRTs of NRC, due to substituting the Xenon Triple Point (XeTP) in place of the Mercury Triple Point (MTP). Top: using the MTP, bottom: using the XeTP. The equations of the ITS-90 are the same in both cases, only the couples (T_{90},W) for the fixed point are changed.
Subrange 1: From the Hydrogen Triple Point to the Water Triple Point,
Subrange 2: From the Neon Triple Point to the Water Triple Point,
Subrange 3: From the Oxygen Triple Point to the Water Triple Point,
Subrange 4: From the Argon Triple Point to the Water Triple Point.

Fig. 7 The effect, in subrange 1, on cSPRT dependence (NU3) due to substituting the XeTP in place of the MTP (see text).

Fig. 8 The propagation of a 1 mK calibration error at the XeTP/MTP fixed point. A comparison of calibration with the XeTP (magenta) vs the MTP (dark blue) for the example of NRC cSPRT 213865.

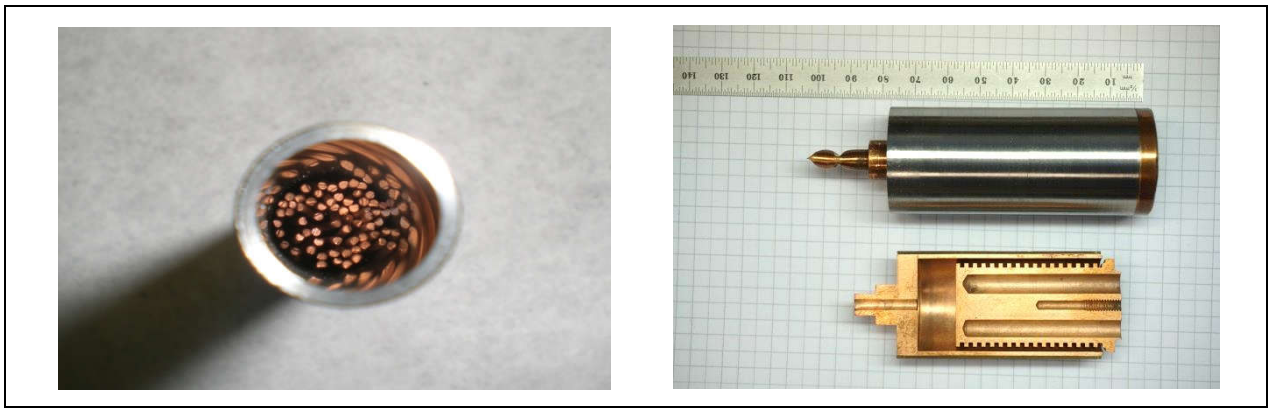

Fig. 1

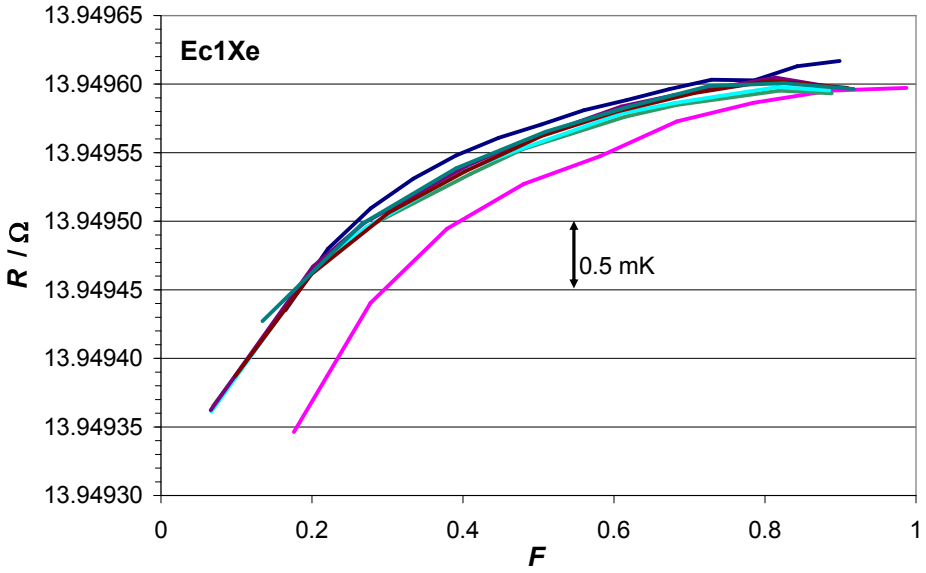
Ec1Xe
13.94965
13.94960
13.94955
13.94950
13.94945
13.94940
13.94935
13.94930
R / Ω
0.5 mK
0
0.2
0.4
0.6
0.8
1
F

Fig. 2

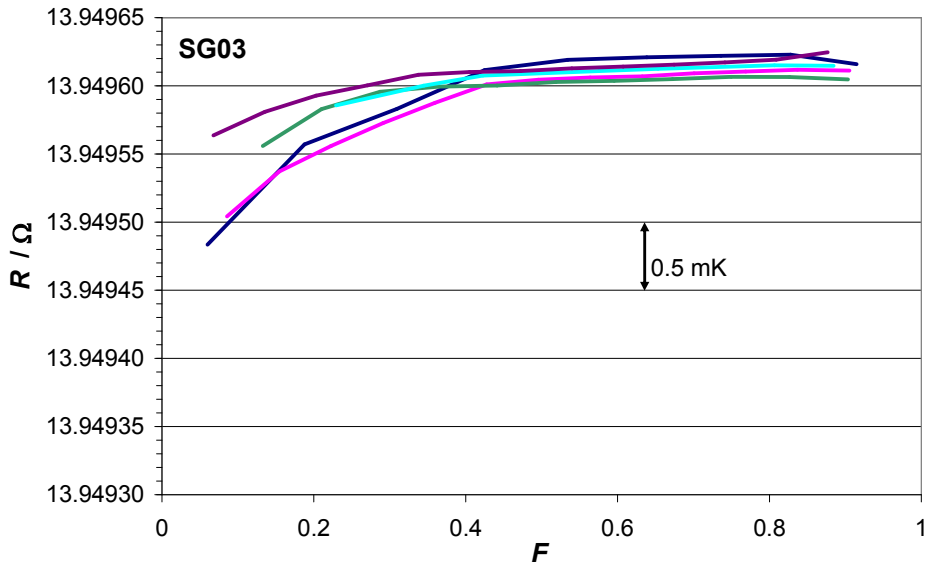
SG03
13.94965
13.94960
13.94955
13.94950
13.94945
13.94940
13.94935
13.94930
R / Ω
0.5 mK
0
0.2
0.4
0.6
0.8
1
F

Fig. 3

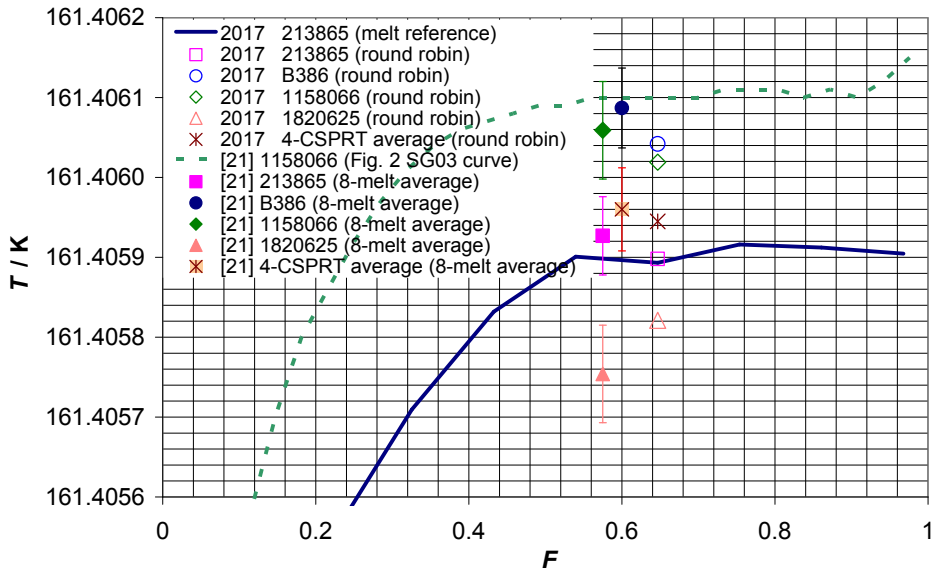
161.4062
161.4061
161.4060
161.4059
161.4058
161.4057
161.4056
T / K
0
0.2
0.4
0.6
0.8
1
F
2017 213865 (melt reference)
2017 213865 (round robin)
2017 B386 (round robin)
2017 1158066 (round robin)
2017 1820625 (round robin)
2017 4-CSPRT average (round robin)
[21] 1158066 (Fig. 2 SG03 curve)
[21] 213865 (8-melt average)
[21] B386 (8-melt average)
[21] 1158066 (8-melt average)
[21] 1820625 (8-melt average)
[21] 4-CSPRT average (8-melt average)

Fig. 4

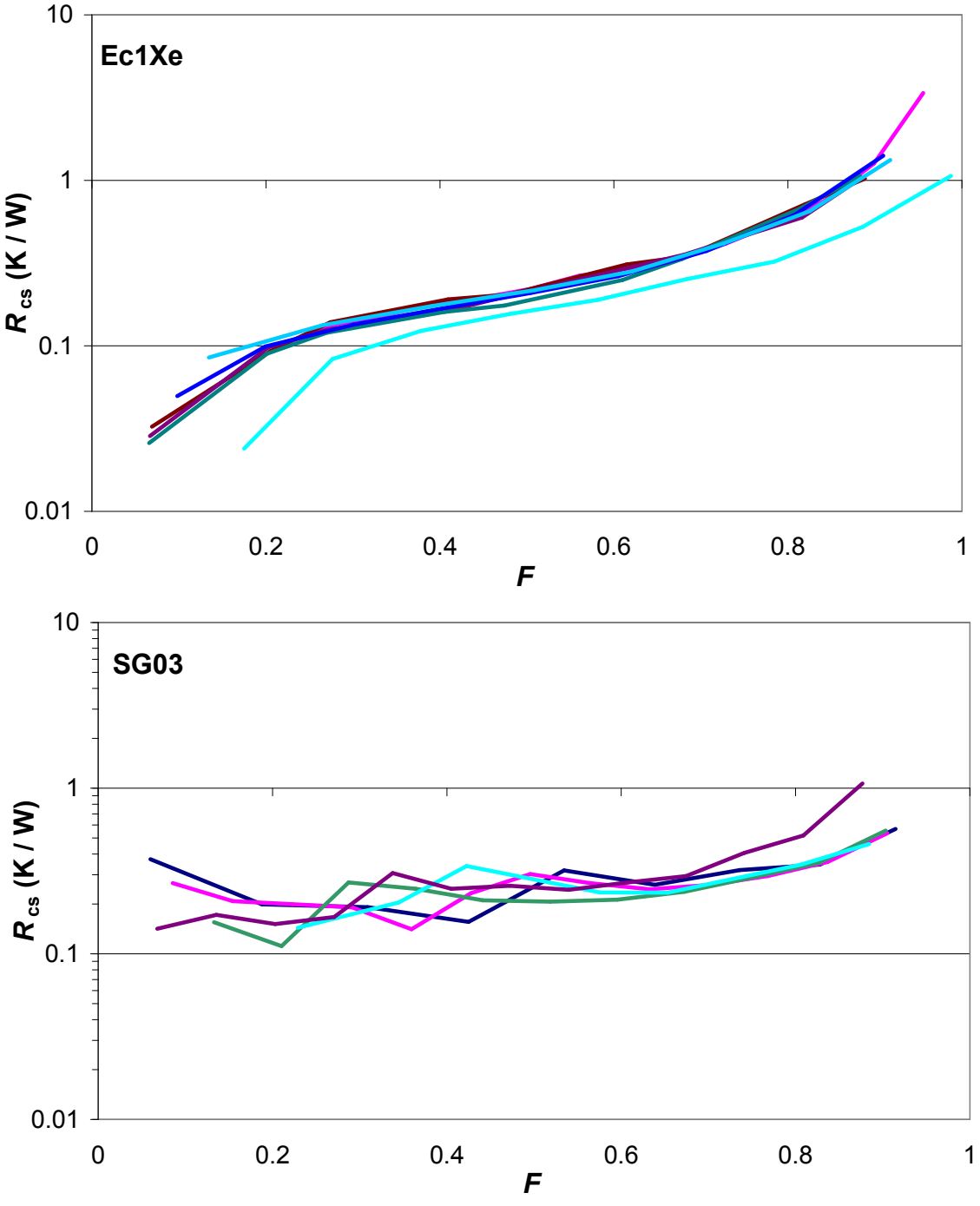
Ec1Xe
10
1
0.1
0.01
R_{cs} (K / W)
0
0.2
0.4
0.6
0.8
1
F
SG03
10
1
0.1
0.01
R_{cs} (K / W)
0
0.2
0.4
0.6
0.8
1
F

Fig. 5

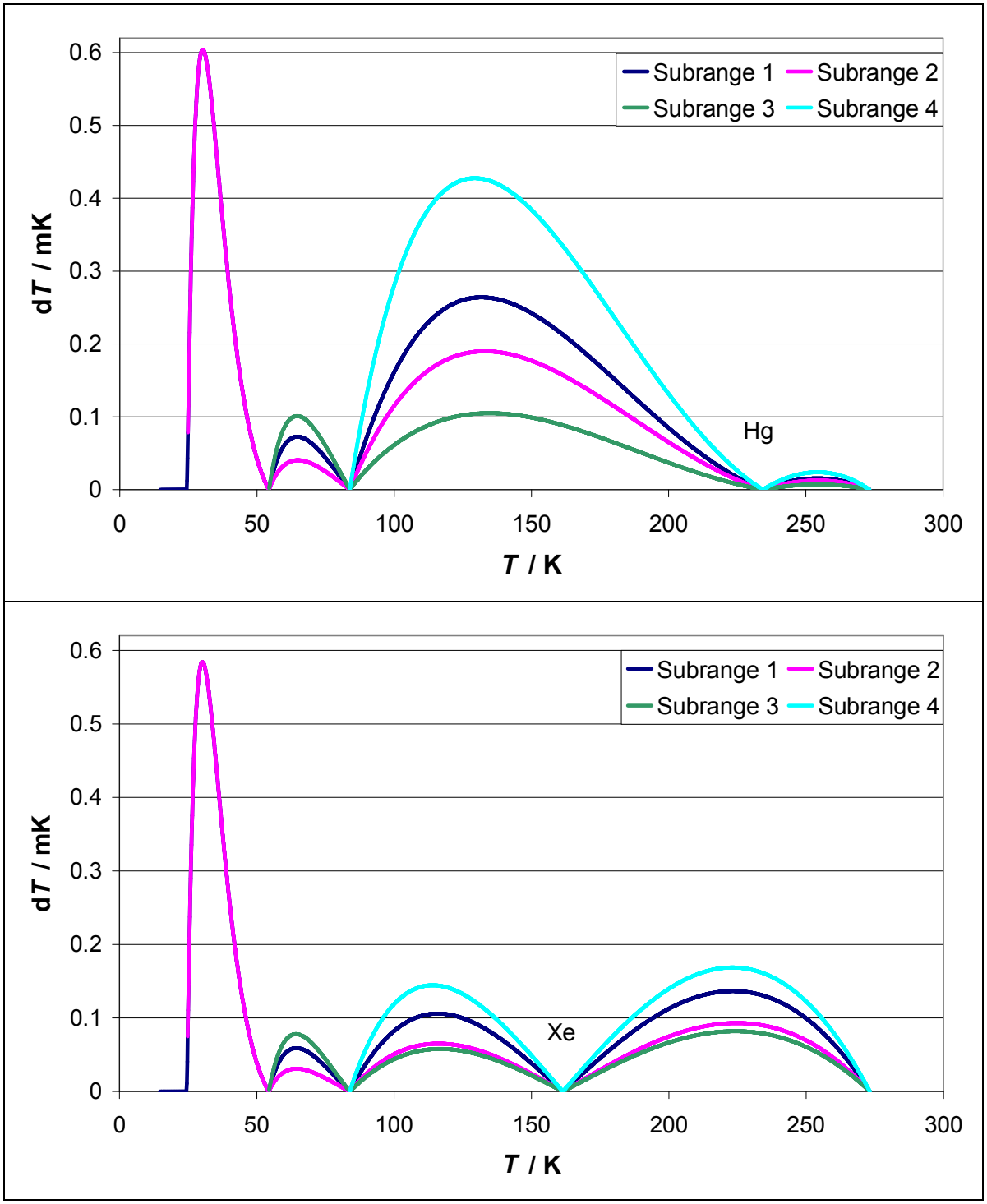
Subrange 1
Subrange 2
Subrange 3
Subrange 4
dT / mK
T / K
Hg
Xe
0
0.1
0.2
0.3
0.4
0.5
0.6
0
50
100
150
200
250
300

Fig. 6

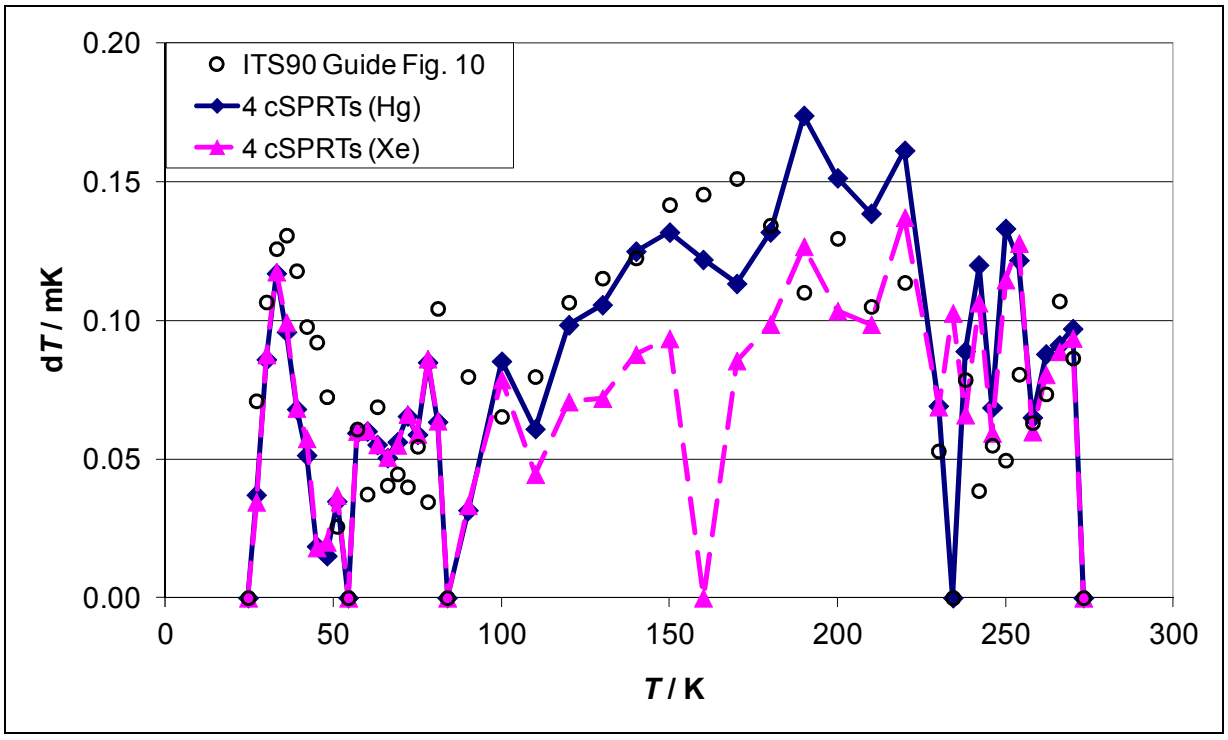
ITS90 Guide Fig. 10
4 cSPRTs (Hg)
4 cSPRTs (Xe)
0.20
0.15
0.10
0.05
0.00
dT / mK
0
50
100
150
200
250
300
T / K

Fig. 7

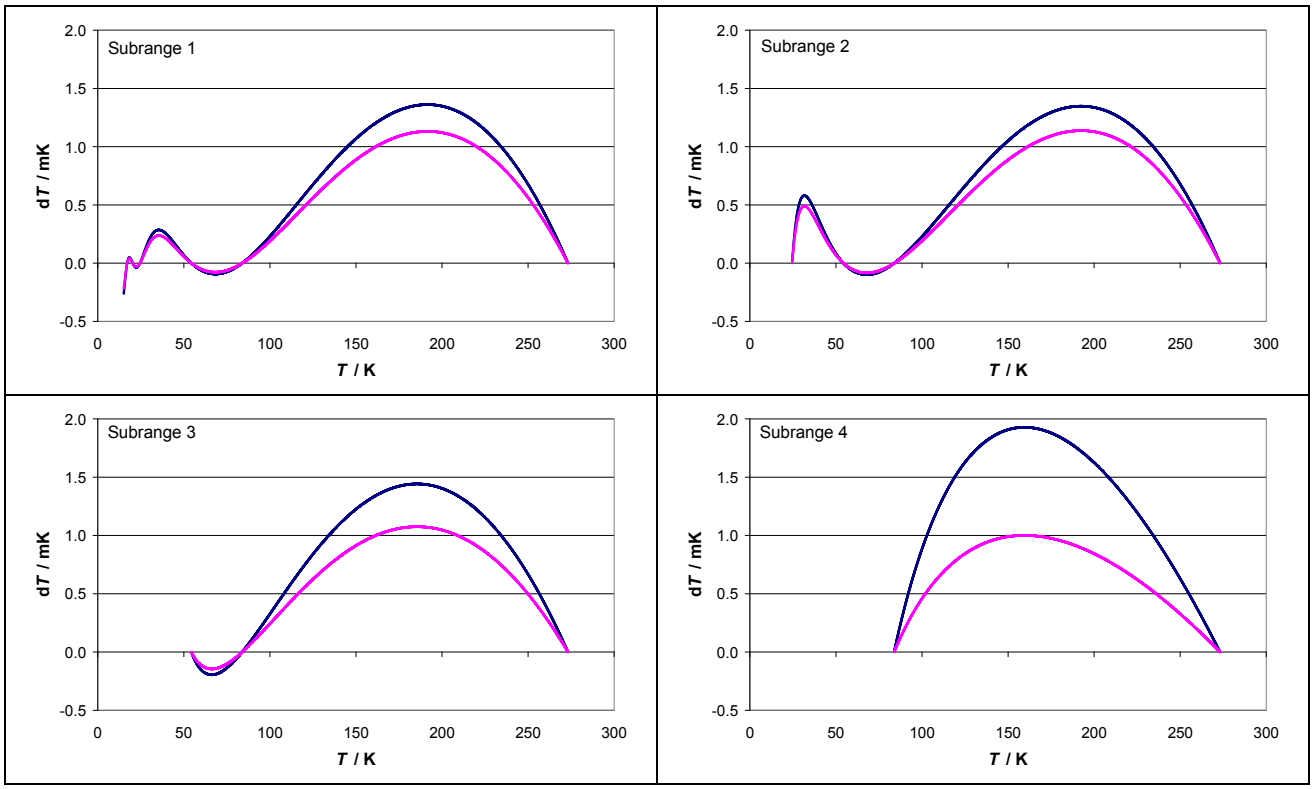
Subrange 1
Subrange 2
Subrange 3
Subrange 4
dT / mK
T / K
2.0
1.5
1.0
0.5
0.0
-0.5
0
50
100
150
200
250
300

Fig. 8